Volume Title
ASP Conference Series, Vol. **Volume Number**
Author
© **Copyright Year** Astronomical Society of the Pacific

arXiv:1405.0600v1 [astro-ph.HE] 3 May 2014

Simulation of microquasars - the challenge of scales

Rolf Walder,[1] Mickaël Melzani,[1] Doris Folini,[1] Christophe Winisdoerffer,[1] and Jean M. Favre[2]

[1]*École Normale Supérieure, Lyon, CRAL, UMR CNRS 5574, Université de Lyon, France*

[2]*CSCS Lugano, Switzerland*

Abstract. We present first results of a long-term project which aims at multi-scale, multi-physics simulations of wind accretion in microquasars and high-mass X-ray binaries. The 3D hydrodynamical simulations cover all scales, from the circum-binary environment down to the immediate vicinity of the black hole. We first introduce the numerical method and parallelization strategy of the AMR A-MAZE code. We then discuss some preliminary results of how, and on what scales, an accretion disk is formed around the black hole. We finally present some characteristics of this disk, which is far from Keplerian. We emphasize that on all scales shocks play a decisive role for the accretion process and the process of structure formation – for the formation of the large scale, nearly coherent structure of the disk, but also for the formation of turbulent fluctuations.

1. Introduction

We want to study wind-accreting microquasars (MQ): accreting black holes (BH) bound to a companion star. This process leads to strong X-ray emission close to the Eddington limit (for a review, see Remillard & McClintock 2006). This puts MQs into the class of X-ray binaries. Accretion into a BH is connected to the launch of relativistic jets, either permanently or episodically (see Fender & Belloni (2004) for a review). This relates MQs to objects like Gamma-Ray Bursts and Active Galactic Nuclei. Non-thermal processes, particle acceleration, and associated γ-ray emission are observed in MQs (a good review is Dubus 2013). The excellent observational coverage and human accessible time-scales, from milli-seconds to years, make MQs an ideal laboratory to study multi-scale and multi-physics processes.

Accretion in MQs takes place either by Roche-lobe overflow (RLOF), or by collecting mass out of the wind of the companion, or by a combination of both. Main sequence low mass companions have only very weak winds, which cannot contribute to the accretion into the BH. Thus, they are pure RLOF systems. Evolved low mass or high mass companions have strong winds, which can significantly contribute to the mass feeding of the BH. In many cases, like for instance in the low mass system GRS 1915+105, hosting a red giant companion, RLOF and wind-accretion operate in common. Finally, there is a class of systems where the high mass companion does not fill its Roche lobe and the BH is fed purely from the companion wind. It is this case which we discuss in this paper.

For our simulations and the results presented here, we take the parameters of the well observed system Cyg X-1 (Orosz et al. 2011). A major issue in wind-accreting systems is how winds are accelerated in the presence of a second ionizing source, the X-rays originating from the vicinity of the BH (Stevens & Kallman 1990; Blondin 1994; Hadrava & Čechura 2012). To keep this first multi-scale study of MQs simple, we decided to ignore this question. Instead, we performed a set of simulations with different constant values for the wind speed: 750 km/s, 850 km/s, 1000 km/s, 1500 km/s, 2000 km/s, and 2500 km/s. We launch the wind with this velocity directly from the surface of the companion star. Another major issue is that radiative transfer effects influence the thermodynamical state of the flow, and subsequently its dynamics. For this first study, we us a simple polytropic equation of state with different indices: $\gamma = 5/3, 4/3, 1.1, 1.01$. An asset of our simulations is, by contrast, their spatial resolution, from the circum-binary scale (computational domain : 10^{14} cm cubed) down to some 10 gravitational radii of the BH ($R_G = 2GM_{BH}/c^2 = 4.4 \cdot 10^6$ cm). This allows, for the first time, to study the accretion wake and the formation of an accretion disk under otherwise idealized conditions. Euler equations are solved. More complex physics and the acceleration process of the wind will be included in future. Also, in this paper, we strictly concentrate on the case of the 750 km/s wind and $\gamma = 1.1$.

In Sect. 2, we present our numerical methods, in Sect. 3 our results, and we conclude in Sect. 4.

2. Numerical method

The simulations were performed with the A-MAZE simulation toolkit (Walder & Folini 2000; Folini et al. 2003; Melzani et al. 2013), comprising 3D parallelized MHD, radiative transfer, and particle in cell plasma codes. For the hydrodynamical simulations we used the explicit multi-dimensional method by Colella (1990), the Riemann solver by Colella & Glaz (1985), and the block-structured AMR algorithm by Berger (1985).

Our adaptive grid is setup similarly as in Walder et al. (2008) (see also Fig. 1). The orbital scale is covered by finer meshes than the circum-binary scale. A nested tree of grids is constructed around the accreting BH moving through the wind of the companion. It is only at this single spot, where many levels of refinement (up to 19 for certain models) are needed to resolve the process of disk formation and to capture the scale of the gravitational radius of the BH. Note that in spatially refined blocks the time-step is adapted as well, such that for all grids the cfl-number can be kept constant. In this way, we are able to resolve time-scales associated to each region in an optimal way. Time steps in the vicinity of the BH are milli-seconds, corresponding to dynamical time-scales in this region (e.g. quasi-periodic oscillations, QPOs). Similarly, time-steps on the orbital scales are of order of a minute. For one orbit of 5.6 days, we need in this way around 10'000 time-steps on the coarsest grid.

Nevertheless, although the code shows very good weak scaling even for fully dynamic AMR if blocks of more than 30^3 cells are used (scaling limit), the setup used here limits the number of processors one can use. In many simulations, fine grids are needed throughout the computational domain, thus dominate the computational costs. Using many processors then reduces the wallclock time if parallelization on the finest level scales optimal - even if coarser levels have some scaling flaws due to too small blocks. However, for the accretion problem, the size (measured in cells) of refined regions is about constant for all levels. The scaling limit thus provides a natural limit of

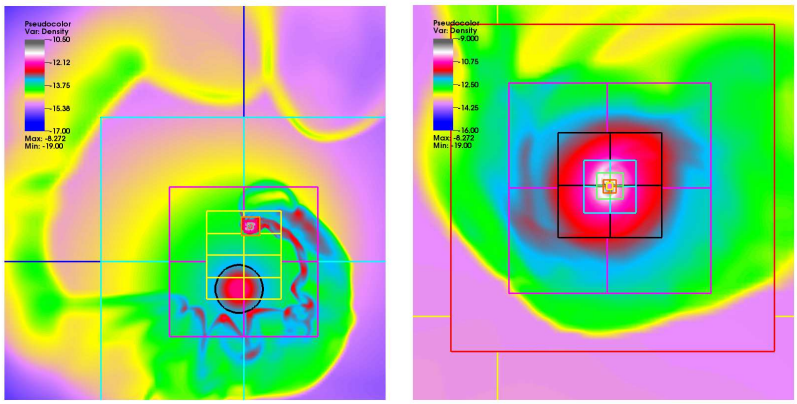

Figure 1. Structure on the circum-binary scale (left panel, $1.5 \cdot 10^{13}$ cm, approximately 1/6 of the computational domain) and on the scale of the bow-shock heading the accretion wake (right panel, $2-3 \cdot 10^{11}$ cm, or approximately $45'000-70'000$ R_G from the BH, the two numbers indicate the fluctuation size). 2D-extracts of density in the orbital plane are shown. The mesh structure with its different levels of refinement is superimposed. The finest level in this case is 14, each level refining by a factor of 2. The radius of the accreting sphere (BH boundary) corresponds to 150 R_G.

parallelization that could only be overcome by improving strong scalability. For this study, we used 8 processors working on 8 blocks of 40^3 cells, resulting in a mesh of about 7 million (14 refinement levels), or 10 million cells (19 refinement levels), respectively. Nevertheless, thanks to larger time-steps on coarser meshes, the net gain in both, CPU and wallclock time is considerable. Scalar computation would result in 8 times more wallclock, non-time adaptivity in much more CPU time to achieve the same result. In a later stage of the study, we may increase the size of refined regions and use 64 processors. Data-files in hdf5 format take 1 to 1.5 GB for one time step.

A final note on numerical methods: the presented problem is hard to resolve on the basis of an explicit solver as time-scales involved span milli-seconds to years. Part of the problem can be overcome by time-step adaption as described above, but the problem remains rather stiff. Implicit solvers could possibly overcome the stiffness, resulting in a net gain of compute time and diminishing use of compute resources. We have started to develop such solvers (Viallet et al. 2011, 2013), which indeed prove to be much faster than explicit solvers. However, these solvers are not yet ready to treat also shock waves, and the solvers are not yet implemented into the AMR code. But these issues should not be principle obstacles for the use of implicit solvers, see Birken (2012) for a review of the newest developments in the field. On the other hand, implicit-explicit schemes may turn out to be an interesting alternative to fully implicit schemes (e.g. Kupka et al. 2012, see also the contribution of F. Kupka in this volume).

3. The $v_W = 750$ km/s multi-scale model: first results

We briefly describe the process driving the nearly spherically symmetric and homogeneous wind of the companion to form an accretion cone, then a subsequent spinning structure around the BH, and finally a non-classical accretion disk close to the BH, at the same time developing turbulent fluctuations on each of these scales.

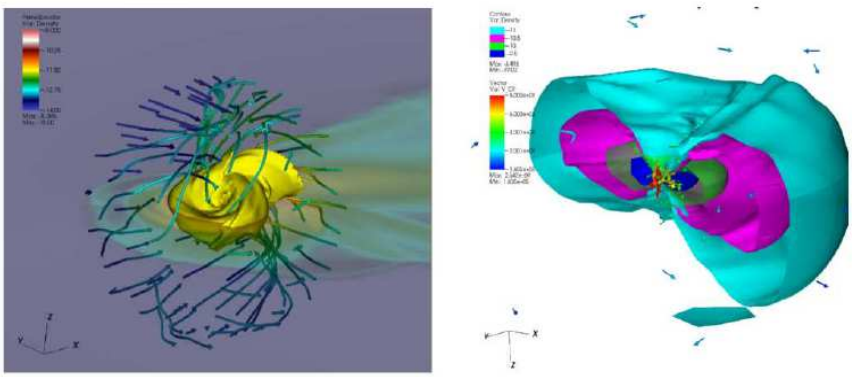

Figure 2. Behind the bow shock, on a scale of $R \approx 50'000\,\mathrm{R}_G$, a spinning structure starts to form (left panel). Shown is density in orbital plane, a 3D density isosurface and the velocity field in streamlines. It is only on a much smaller scale, on a scale of about $5'000\,\mathrm{R}_G$, where the spinning structure is flattened to form a disk (right panel). Shown here are different density isosurfaces and the flow field in vectors.

The large scale, circum-binary structure of the system is dominated by the spirally-shaped accretion-cone trailing the bow-shock around the black hole (Fig. 1, left panel). Though only the part very close to the BH is involved in the accretion process, the enhanced density of this cone may lead to non-negligible absorption processes observable in the binary spectrum, causing either secondary dimming or even occultation of the X-ray source (Dumm et al. 2000; Goldstein et al. 2004).

Closer to the BH, to about half the Bondi-Hoyle accretion radius or $45'000$ – $70'000\,\mathrm{R}_G$, a bow-shock forms in front of the BH moving on its orbit through the wind (Fig. 1, right panel). The bow shock is highly variable in time and space, mostly due to turbulent fluctuations in the wake. The shape-variations of the shock itself force the turbulence (Foglizzo 2002; Folini & Walder 2006). The shocked material is immediately re-accelerated by the gravitational field of the BH. It collides with other material falling in the accretion cone towards the BH. The net angular momentum of these converging flows lets arise a structure that spins pro-grade around the BH. We emphasize that a substantial part of the angular momentum is dissipated in the many shocks that accompany the merging of these different colliding flows. The spinning structure on this scale bares no resembling with a disk. It is still an essentially 3D structure interwoven with strongly varying shocks and showing strong discontinuities in all flow variables (Fig. 2, left). Shocks play an important role in the transport of angular momentum down to the BH scale.

In each shock passage, the falling material looses angular momentum. This causes a flattening and circularizing of the flow. Shocks become steadily more coherent. In the inner part, shocks are 1- or 2-armed spirally-shaped waves, whose positions only evolve on secular time scales. In this hydrodynamical model, the emerging disk is neither thin nor Keplerian (Fig. 2, right), but nevertheless a disk which may emit not too differently from a Keplerian disk. The heating process, however, is dominated by shocks rather than viscous shear, though this second process certainly also plays a role. Density and velocity fluctuations within the disk are still of order 20–30 percent. The thickness of the disk is essentially given by the pressure of turbulent fluctuations within the disk and

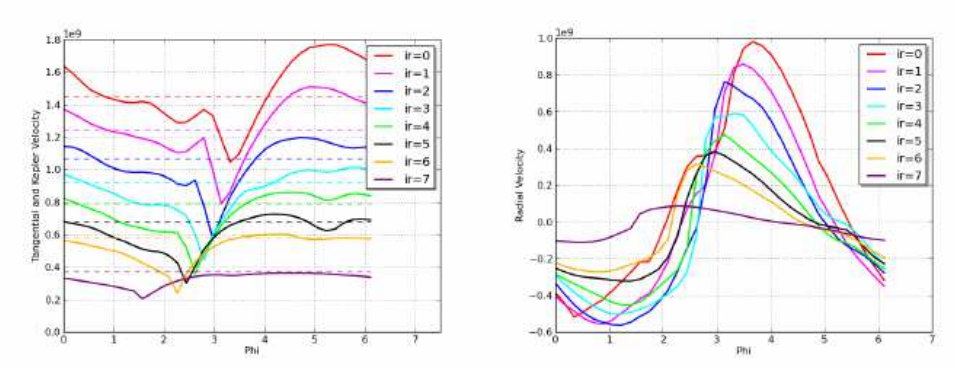

Figure 3. Tangential (left panel, together with Kepler velocity) and radial component (right panel) of the velocity [cm/s] in the central plane of the disk, shown for different radii of the disk (214 R_G (ir=0), 290 R_G, 393 R_G, 531 R_G, 720 R_G, 976 R_G, 1322 R_G, 3286 R_G (ir=7)). Positive tangential velocity indicates a pro-grade rotation of the disk (i.e. particles move from small to large ϕ). Positive radial velocity indicates a movement towards the BH. The spiral shock wave is visible as minima of the tangential velocity / maxima of the radial velocity, shifting with the radius. Velocity components normal to the disk have values of the same order.

the kinetic pressure built up by the material steadily raining down on the disk from flow features above and below the disk. In some cases, shocks in the down-draining material can build up, confining the disk. Both, turbulent fluctuations and the down-drain of material, may cause flickering of the emission as observed in many wind-accreting X-ray binaries.

Fig. 2, right, demonstrates that the disk is not symmetric, but has a larger scale-height in its right part. Also, the disk is occasionally warped and/or tilted against the orbital plane. However, we cannot yet exclude that this is an artifact of non-relaxed initial conditions. Fig. 3 illustrates both, the velocity variations within the disk (along imaginary circular orbits for different radii) and angular momentum advection by spiral shocks. Clearly, flow motion is not at all along circular orbits, as indicated by the strong smooth variation of the tangential and radial velocity components. The velocity components also change abruptly. Each shock passage decelerates the fluid parcel, breaking the tangential flow component, the centrifugal force is diminished, gravity acts, acceleration towards the BH occurs. In Fig. 3, the spiral shock is visible as points of smallest tangential velocities and largest radial velocities, shifting with radius.

4. Discussion and Conclusions

We presented first results of our project on multi-scale, multi-physics simulations of microquasars. We first discussed the efficiency of parallel computation of time-adaptive AMR simulations using many levels of refinement at one spatial spot only. We then presented a preliminary analysis of how a disk is formed out of the 3D flow accreting material from a wind shed by the companion star. We note that such a disk is not always formed. Depending on the wind speed of the companion, the 3D structure of the accretion flow may be essentially conserved down to the scale of the gravitational radius of the black hole. Angular momentum is advected by a network of shocks. This

is similar to what has been discussed by Walder et al. (2010) for the low mass binary case, where we called this case the accretion ball regime (see also Mitsumoto et al. 2005). For very high speed winds, we find stable disks which are rotating retrograde. A more thorough discussion of these other accretion regimes will be published elsewhere.

As perspective we note that a similar study is in preparation for the MHD case. With this forth-coming study, we hope to learn more on whether magnetic fields essentially change the disk-formation process. Certainly one expects another essential heating process to be present, magnetic reconnection. On a longer time scale, we want to combine MHD simulations with kinetic simulations and radiative transfer.

Acknowledgments. We acknowledge support from the French Stellar Astrophysics Program PNPS and computing time from the Grand Equipement National de Calcul Intensif (GENCI), project number x2012046960 and support from the Pôle Scientifique de Modélisation Numérique (PSMN) at ENS-Lyon.

References

Berger, M. J. 1985, Lectures in applied Mathematics, 22, 31
Birken, P. 2012, Numerical methods for the unsteady compressible Navier-Stokes equations, habilitation thesis (online: http://www.mathematik.uni-kassel.de/ birken/)
Blondin, J. M. 1994, ApJ, 435, 756
Colella, P. 1990, J. Comp. Phys., 87, 171
Colella, P., & Glaz, H. 1985, J. Comp. Phys., 59, 264
Dubus, G. 2013, A&A Rev., 21, 64
Dumm, T., Folini, D., Nussbaumer, H., Schild, H., Schmutz, W., & Walder, R. 2000, A&A, 354, 1014
Fender, R., & Belloni, T. 2004, ARA&A, 42, 317
Foglizzo, T. 2002, A&A, 392, 353
Folini, D., & Walder, R. 2006, A&A, 459, 1
Folini, D., Walder, R., Psarros, M., & Desboeufs, A. 2003, in Stellar Atmosphere Modeling, edited by I. Hubeny, D. Mihalas, & K. Werner, vol. 288 of Astronomical Society of the Pacific Conference Series, 433
Goldstein, G., Huenemoerder, D. P., & Blank, D. 2004, AJ, 127, 2310
Hadrava, P., & Čechura, J. 2012, A&A, 542, A42
Kupka, F., Happenhofer, N., Higueras, I., & Koch, O. 2012, Journal of Computational Physics, 231, 3561
Melzani, M., Winisdoerffer, C., Walder, R., Folini, D., Favre, J. M., Krastanov, S., & Messmer, P. 2013, A&A, 558, A133
Mitsumoto, M., Jahanara, B., Matsuda, T., Oka, K., Bisikalo, D. V., Kilpio, E. Y., Boffin, H. M. J., Boyarchuk, A. A., & Kuznetsov, O. A. 2005, Astronomy Reports, 49, 884
Orosz, J. A., McClintock, J. E., Aufdenberg, J. P., Remillard, R. A., Reid, M. J., Narayan, R., & Gou, L. 2011, ApJ, 742, 84
Remillard, R. A., & McClintock, J. E. 2006, ARA&A, 44, 49
Stevens, I. R., & Kallman, T. R. 1990, ApJ, 365, 321
Viallet, M., Baraffe, I., & Walder, R. 2011, A&A, 531, A86
— 2013, A&A, 555, A81
Walder, R., & Folini, D. 2000, in Thermal and Ionization Aspects of Flows from Hot Stars, edited by H. Lamers, & A. Sapar, vol. 204 of Astronomical Society of the Pacific Conference Series, 281
Walder, R., Folini, D., Favre, J. M., & Shore, S. N. 2010, in Numerical Modeling of Space Plasma Flows, Astronum-2009, edited by N. V. Pogorelov, E. Audit, & G. P. Zank, vol. 429 of Astronomical Society of the Pacific Conference Series, 173
Walder, R., Folini, D., & Shore, S. N. 2008, A&A, 484, L9